

SIMULATION AND OPTIMIZATION OF A SLURRY-BASED FIBERGLASS PREFORM MANUFACTURING PROCESS

Richard W. Johnson
Mark D. Landon
Idaho National Engineering Laboratory
Idaho Falls, Idaho

DISCLAIMER

This report was prepared as an account of work sponsored by an agency of the United States Government. Neither the United States Government nor any agency thereof, nor any of their employees, makes any warranty, express or implied, or assumes any legal liability or responsibility for the accuracy, completeness, or usefulness of any information, apparatus, product, or process disclosed, or represents that its use would not infringe privately owned rights. Reference herein to any specific commercial product, process, or service by trade name, trademark, manufacturer, or otherwise does not necessarily constitute or imply its endorsement, recommendation, or favoring by the United States Government or any agency thereof. The views and opinions of authors expressed herein do not necessarily state or reflect those of the United States Government or any agency thereof.

MASTER

ABSTRACT

As a part of the Partnership for a New Generation of Vehicles (PNGV) program directed by the U.S. Department of Commerce, the U.S. Department of Energy (DOE) is currently supporting various research and development projects identified by representatives of the U. S. Council for Automotive Research (USCAR) as high priority areas deserving special attention. A water-based slurry process for producing chopped fiberglass preforms that can be used in manufacturing structural automotive composites is being developed by researchers at the Idaho National Engineering Laboratory (INEL) and members of the Automotive Composites Consortium (ACC), as part of the U. S. Advanced Manufacturing Partnership (USAMP). The main objective of the project is to achieve a uniform (by mass) distribution of fibers in the preform. To this end, computer modeling and experimental efforts are currently underway at the INEL. The present article reports strategy, progress and current results for the modeling effort. The modeling effort includes computational fluid dynamic simulations of the current process to help visualize process dynamics and computer-based design optimization that automatically adjusts process parameters to find the best design to meet the objective.

INTRODUCTION

An important goal of the Partnership for a New Generation of Vehicles (PNGV) program of the U.S. Department of Commerce is to increase the gas mileage of future U.S. made automobiles. One method of accomplishing this task is to decrease the weight of the vehicle. Lightweight composites are currently under development for use for various automobile components. Automobile components come in a variety of shapes and sizes, requiring that the composite materials be manufactured in complex shapes and sizes. For fiberglass composites, this means that fiberglass mattes or preforms must be formed into complex shapes before being used in the manufacturing process.

One way to form fiberglass preforms into complex shapes is to press a thermo-plastic-fiber-laced fiberglass blanket into a complex-shaped mold using heat and pressure to achieve the desired matte density and set the thermo-plastic fibers to maintain the shape. While this method is feasible, it creates significant waste as the blankets are trimmed to the appropriate shapes. Another method for creating preforms in the desired shape that can produce high-densities and can reduce waste to negligible levels, is a slurry tank method. The slurry tank is a large cylindrical tank filled with water with a hydraulically driven piston as shown in Figure 1. A screen having the desired preform (matte) shape is secured in the center of the piston. After charging the tank with chopped fiberglass and thermo-plastic fibers and mixing them into the water with air jets issuing from the top of the piston, the piston is moved upward such that the water and fiberglass slurry is forced through the screen. After the slurry passes through the screen, a mating screen is placed on top of the first screen; the screens and matte are taken to a drier and dried to set the thermoplastic fibers such that the preform shape is set.

The slurry tank method for manufacturing fiberglass preforms, being developed by The Budd Company of Warren, MI, has not progressed to the point that the preforms created are of

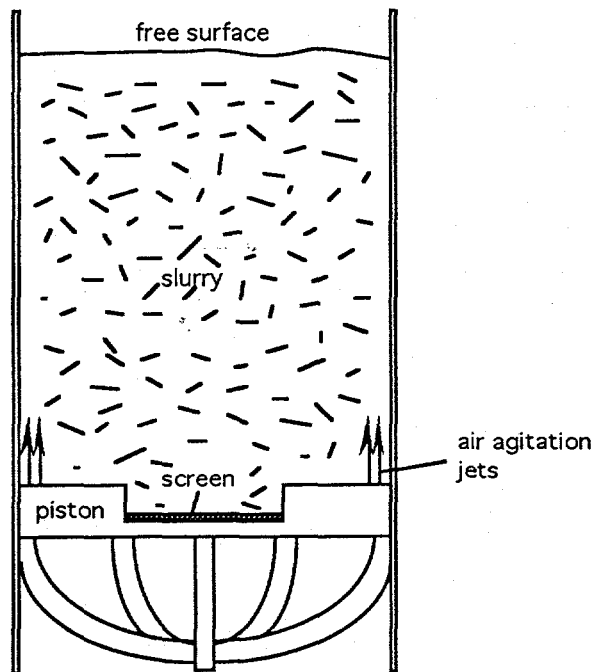


Figure 1. Schematic of slurry tank showing hydraulically driven piston in starting position, air agitation jets and screen.

sufficiently uniform density. That is, the slurry process currently produces preforms, even for flat screens, that vary in density as a function of location on the surface of the preforms. For a flat, square test screen, the outer edges of the preforms tend to have excessive fiberglass buildup, while too few fibers are deposited in the center.

The goal of the project is to determine which parameters are important to the slurry process and how they may be controlled to minimize the variation of fiber density in the preform. The strategy to accomplish this goal is three-fold: 1) a modeling effort using computational fluid dynamics (CFD) software to simulate the flow patterns in the slurry to help visualize and understand the physics of the process, 2) application of optimization software along with the analysis software to find optimal values of design parameters and 3) an experimental effort to accompany the modeling effort to help validate the modeling and bring to light physics that may be missed by the modeling. The present article reports on the progress of the modeling and optimization efforts and what has been learned to date. We caution that the results reported are only preliminary and should not be viewed as the final conclusions of the program. We next describe the strategy and objectives of the modeling plan.

MODELING PLAN

The production of the glass-fiber preform involves the complex transient, multiphase, multicomponent flow of water, air bubbles and solid fibers in a slurry tank with a free surface. The solid fibers are a dilute suspension of chopped fiberglass lengths that have the appearance of blades of grass. The fiberglass strands are connected in bunches, having the form of "blades" that are several strands wide, one or two strands thick and are cut into lengths on the order of two or three inches. The most general model that could be used to model such a slurry would have to account for the fluid dynamics of the water, the effects of the water on the fiberglass strands and the effects of the fiberglass strands on the water. Furthermore, the model would have to account for the effects of buildup of the fibers on the screen since this affects the flow of the water through the screen.

A recent paper by Baloch and Webster¹ on the flow of fiber suspensions in a Newtonian solvent (such as water) indicates that if the overall Reynolds number of the flow is above 20, the fibers have no effect on the fluid dynamics of the water. The Reynolds number of the flow in the slurry tank relative to the piston is on the order of 150,000, meaning that the fibers have virtually no influence on the fluid dynamics of the water. In considering the effects that the water has on the fibers, we note that the density of the fiberglass is about 20 - 25% greater than that of the water. Because the fiberglass density is quite close to that of water and because the dynamics of the water is so vigorous, we believe that the fibers simply follow along the same flow paths as the water most of the time. Unfortunately, since the fibers are fibers and not spheres, they may also tend to wrap around each other and be tugged by water moving at different velocities at different points. We believe that modeling these effects is probably not very important for the slurry process and that a suitable model can ignore these effects. The validation of this assumption may be apparent after the development of the process is completed.

The simplified approach that we have determined to use is to assume a single-phase, single-component flow. We solve the normal incompressible equations of fluid dynamics. We neglect the presence of fibers in the bulk of the water except that we model their deposition on the screen by assuming the presence of a porous medium whose thickness varies with time. We assume that the local deposition rate of fibers on the screen is proportional to the local flow rate of water through the screen. We also assume that the slurry is well-mixed, that is the fibers are uniformly distributed in the water. Finally, we model the air jets as water jets to remove the air phase.

The domain encompassed by the simulation includes regions above and below the piston. We model the screen as a porous medium; however, we had to determine the permeability of the screen in order to use a porous flow model. The several objectives of the modeling effort are outlined below along with sub-objectives that were seen as necessary to achieve a main objective.

1. Model the three-dimensional steady-state problem where the fluid moves down the cylindrical tank and through a square screen (1.17 m square) for a stationary piston without fiber deposition, jet agitation, or a free surface. The screen should be modeled as a porous medium and the fluid flow below the screen included in the computational domain. The mass flux through the screen should be mapped to see if there are any trends that correlate with the fiber deposition as found experimentally by The Budd Co. The commercial fluid dynamics code FIDAP (Fluid Dynamics International, Inc. Evanston, IL, versions 7.0, 7.5) is chosen for the modeling effort. The following sub-objectives are deemed necessary in order to achieve objective 1.
 - a. Determine the permeability of the screen by modeling the detailed flow of water in a straight pipe with an orifice representing the screen, the orifice having the same open area relative to the pipe as the screen.
 - b. Ensure that the permeability produces the same pressure drop predicted by the porous flow equation of Forchheimer; also, validate the value of permeability for the screen from experimental data.
 - c. Build a two-dimensional axisymmetric model (round screen) to see how well the code simulates the flow using the porous flow model for the screen.
2. Model the three-dimensional problem where the fluid moves through a rectangular screen in a stationary piston in a vertical cylinder with water jet agitation but without fiber deposition or a free surface.
3. Model the three-dimensional unsteady problem where the fluid moves through a rectangular screen in a stationary piston in a vertical cylinder with water jet agitation and fiber deposition but still no free surface. The buildup of the fibers on the screen makes the problem unsteady as the fiber mat will be modeled as a porous medium with time-varying thickness. The permeability of the mat will need to be determined experimentally.
4. Model the three-dimensional unsteady problem where the piston moves through a stationary vertical tank with water jet agitation, fiber deposition and with a free surface.
5. Determine the feasibility of employing optimization technology in connection with the modeling analysis to automatically determine the optimal screen hole spacing.
6. Determine how to connect the output of CAD software that defines a complex shape to FIDAP to allow the generation of the modeling mesh for the particular complex shape.

We next discuss the efforts that have been made to achieve the above objectives, the results, the problems encountered and the lessons learned.

DETERMINATION OF SCREEN PERMEABILITY

Determination of the permeability of the screen as a function of the open area of the screen represents sub-objective 1a. The permeability of the screen is defined based on a porous flow model that is in common use today. The porous flow model used in FIDAP is a variation of

Darcy's equation. A term has been added for large-Reynolds-number porous flow, which is true for our flow; that is, an inertial term has been added to the usual viscous term. The equation is called Forchheimer's equation and is given by ²

$$u \left[\frac{\mu}{\kappa} + \frac{C_E \rho}{\kappa^{1/2}} |u| \right] = - \frac{dp}{dx} \quad (1)$$

where ρ is the density, u is the volumetric flow rate per unit cross-sectional area (or velocity), μ is the dynamic viscosity, C_E is the Ergun coefficient, set to 0.55, κ is the permeability, p is the pressure and x is the flow direction. The first term on the left hand side is the viscous term; the second is the inertial term. Since we know the density, the viscosity (water at 15 °C) and specify the velocity, we can back out the permeability if we know the pressure drop across the screen. We assume that all of the pressure drop occurs within the width of the screen, even though the pressure actually drops quite dramatically and then recovers somewhat over a distance several times the screen width. Hence, we model the flow across the screen at a given velocity and then use FIDAP to compute the pressure drop. Initially, the screen whose permeability we attempted to determine was 1.93 mm thick with holes, diameter 4.7 mm, spaced 6.35 mm apart in a staggered fashion; the open area of the screen was 50%. The velocity of flow through the screen was to be in the range of 0.5 to 1.25 m/sec.

Several questions regarding the flow of water through the screen are important. Is the flow laminar or turbulent; is it steady or unsteady? How fine a mesh is needed? Can we model the three-dimensional geometry accurately? After much effort, we determined that the flow is unsteady, but laminar, at least in the regions of primary interest: upstream of the screen. At first, we tried to use a three-dimensional model of the screen for the flow through just one hole; the screen has hexagonal symmetry. We found that the computing time for the three-dimensional model was so extended that we couldn't use a fine enough mesh to obtain accurate solutions. This conclusion was deduced from experimental data which eventually became available from our experimentalist colleagues. We finally determined that we could achieve accurate pressure-drop data by building a two-dimensional axisymmetric model of flow in a frictionless pipe with an orifice, representing the screen hole. The open area of the orifice with respect to the pipe cross-sectional area was matched to the open area of the screen. With this two-dimensional model, the computational mesh could be refined to the point that the computed data matched the experimental data. The difference between the 2D model and reality was simply that the modeled tube was cylindrical while in reality, a frictionless hexagonal tube was called for. Apparently, the difference in the two geometries was insignificant as far as simulating the pressure drop.

Figure 2 plots the history of pressure drop across the orifice. The flow clearly becomes unsteady. We can see that the unsteady numerical data of Fig. 2 fairly evenly bracket the experimental value of 5885 Pa. The flow velocity was 1.279 m/sec. Figure 3 plots the time-average pressure drop across the screen hole as a function of inlet velocity for the experimental and numerical data; also, the pressure drop predicted by the Forchheimer equation for experimentally and numerically determined permeability is plotted. The experiments were not sensitive to the high-frequency fluctuations seen in Figure 2. The experimental permeability value of $1.0334 \times 10^{-7} \text{ m}^2$ is used in subsequent simulations. This value is the average of the experimental data points seen in Figure 3 (but plotted as u vs. pressure drop). Other screens with different open areas were also subjected to experiment to determine their effective permeabilities.

Sub-objective 1b was completed by building a simple model of flow through a channel with a porous entity with the above permeability and demonstrating that the same pressure drop was computed as is given by the experimental data. To complete objective 1 of the modeling plan, two- and three-dimensional simulations of the tank were performed as described in the next section.

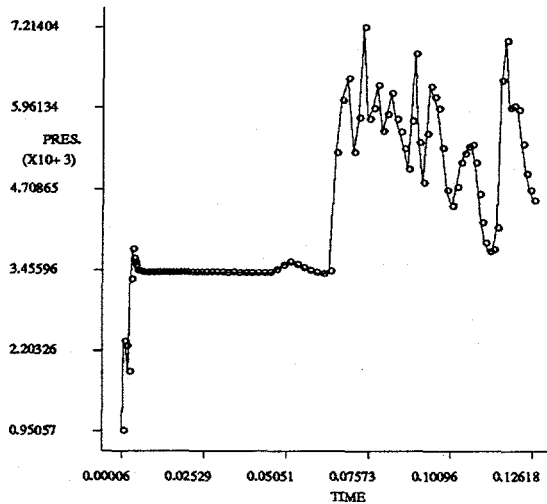


Figure 2. History of pressure drop across orifice as computed numerically. Experimental data give an average pressure drop of 5885 Pa.

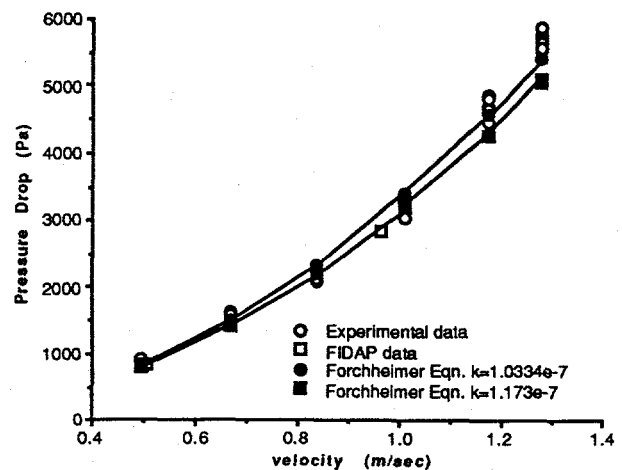


Figure 3. Time-average pressure drop across screen vs. velocity for measured, computed data; using Forchheimer's equation.

SIMULATION OF SLURRY TANK FLOW

Simulation of the flow of the water and fiberglass through the slurry tank was planned to be accomplished through a series of steps as indicated by the modeling plan above. The first step is given by objective 1 and sub-objective 1c of the modeling plan.

SIMULATION OF 2D AND 3D FLOW WITH NO JET AGITATION, FIBER BUILDUP OR FREE SURFACE is the first step toward full simulation of the slurry flow in the tank. Here we assumed that water moved toward a stationary piston at an inlet rate that matched the actual piston speed (0.0762 m/sec). We also assumed that the flow along the tank walls was frictionless, since in reality it is the piston that is moving through the water. We further assumed that the flow was laminar and, of course, that the screen was a porous medium with permeability determined as explained above. It makes sense to assume the flow to be laminar because, except for flow induced by the agitation jets, the slurry is stationary relative to the tank.

Figure 4 shows the finite element grid and a streamline contour plot of the 2D simulation. In Fig. 4a we see the fineness and distribution of elements for the 2D simulation. Figure 4b shows that a recirculation zone is caused by the flow as it pours over the edge of the recess above the screen. The presence of this recirculation affects the distribution of the axial flow as it encounters the screen. Figure 5a shows pathlines for spherical particles injected into the flow at the inlet at the top of the tank. These particles were assumed to have the same density as the fiberglass (specific density 1.23). We see that the particle paths are affected by the recirculation zone such that none make it all the way back around the zone to the wall to which the screen is attached, causing bunching a short ways away from the wall. This effect is partly due to the recirculation zone and partly to the higher density of the particles which causes them to be drawn downward by gravity rather than to follow the streamlines all the way back to the wall. Figure 5b is a line plot of the axial velocity just as it encounters the screen. We see that a very gradual rise in the velocity magnitude occurs moving from the screen center (at the left) toward the outer edge of the screen.

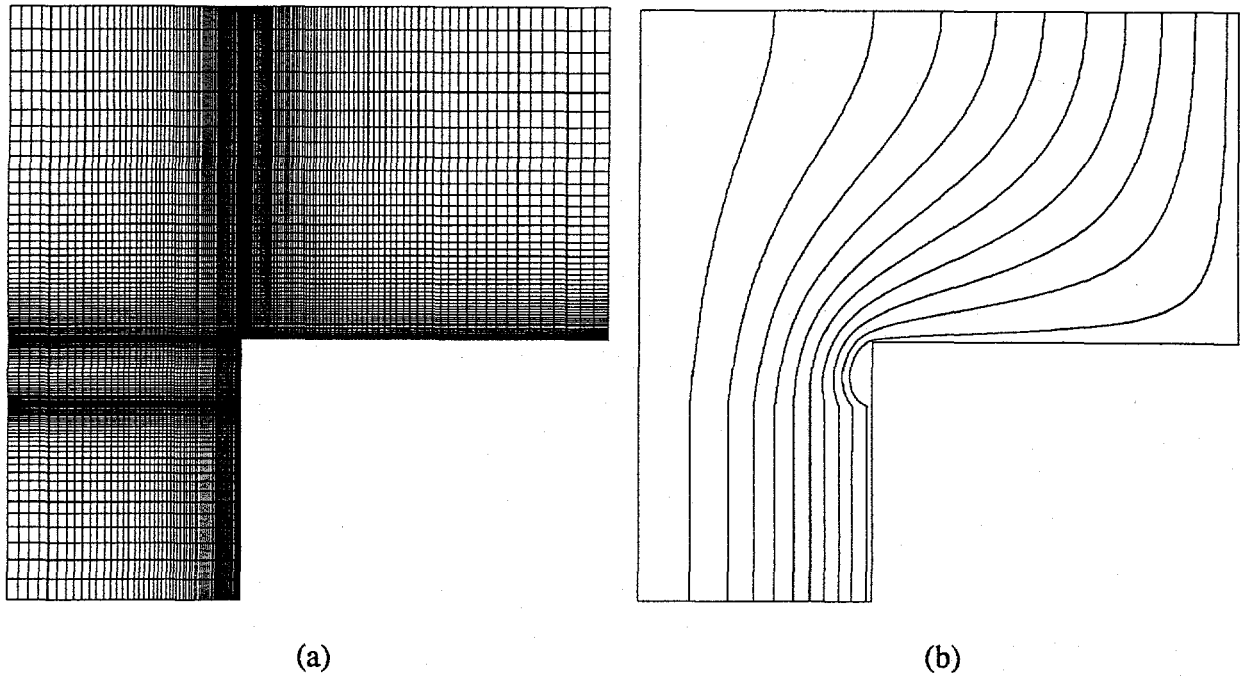


Figure 4. (a) Finite element grid and (b) streamline contours for 2D simulations of slurry tank for objective 1c. Note recirculation zone (bubble) adjacent to recess wall just above screen.

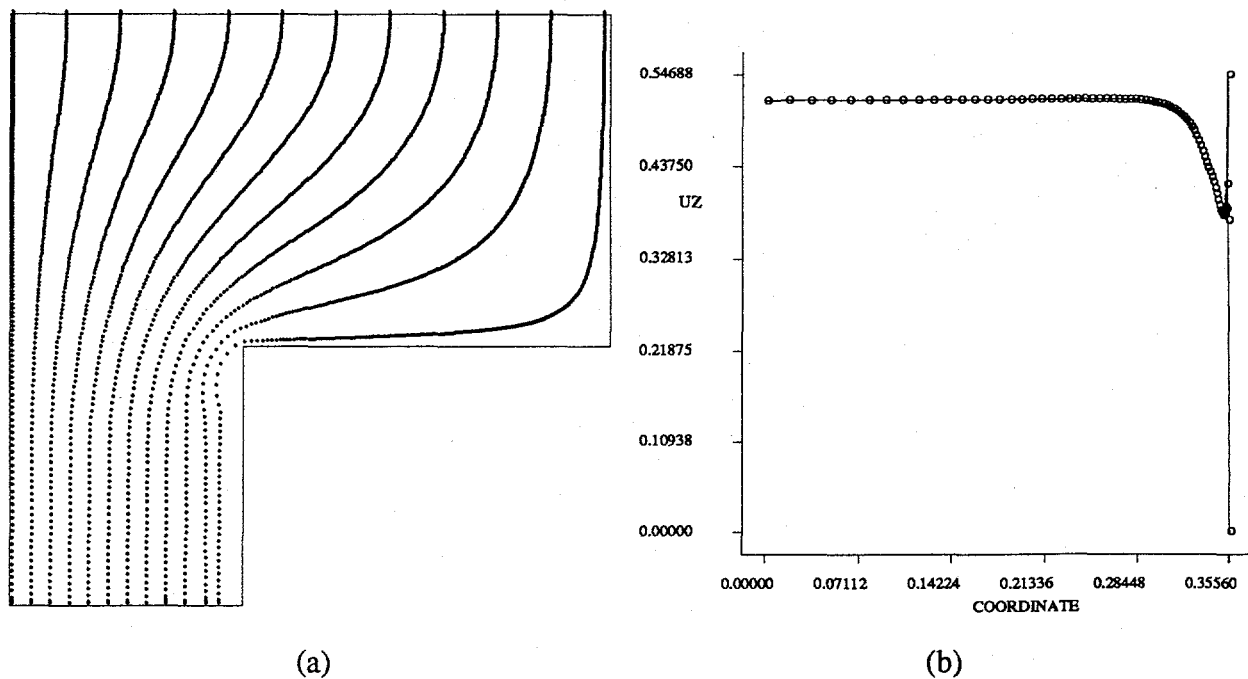


Figure 5. (a) Pathlines of spherical particles seeded into top of 2D slurry flow for objective 1c; note how the particles move around the recirculation zone (see Fig. 4b). (b) Distribution of axial velocity just at the upper face of the screen. The center of the screen is toward the left.

The velocity drops to zero at the outer edge of the screen as dictated by the boundary condition. The 2D computations required about 65 minutes of computing time on a DEC Alpha workstation.

We would conclude from these results that if the fiber deposition on the screen is directly proportional to the mass flow rate of the water through the screen, we would see a low deposition rate adjacent to the wall, but with the highest deposition rate a short ways from the wall where the effects described above cause a peak in the velocity. This conclusion is in direct contrast to experimental results obtained by The Budd Company; of course, we realize that the model is not yet complete.

The effects of three-dimensionality were addressed by a 3D simulation using the same assumptions as for the 2D computations just described. After a number of attempts to produce a 3D simulation, a converged solution was obtained on a grid that was significantly coarser than for the 2D case. Due to symmetry, only a 45 degree sector of the 3D tank was needed for the simulation. Figure 6a illustrates the 3D finite element grid. Figure 6b is a vector velocity plot of the view along one side of the sector (the side in full view in Fig. 6a). We see a flow pattern similar to the 2D results with a recirculation zone occurring just where the water pours into the recess containing the screen. Figure 7a is a contour plot of the axial velocity just as it encounters the screen. We see that the axial flow decreases at the outer screen edge (to zero) and that a larger region of diminished flow rate occurs in the corners of the screen. This would lead us to conclude that the fiber thickness in the corners would be relatively less than farther away from the screen edge, again in contrast to actual data. Figure 7b is a line plot of axial velocity along the edge of the sector that appears to the left as seen in Fig. 7a. Note that the direction of the axial velocity for the 3D model is positive in a direction opposite to gravity; hence, the velocity magnitude is negative as shown in the plot. We see that the axial velocity magnitude increases moving from the screen center (at the left) toward the outer edge of the screen until just before reaching the wall where the velocity drops to zero. This latter result is the same as we found for the 2D case. We conclude that effects not included for this step must be important.

We note that computation time for the 3D results was approximately 110 hours on the same DEC Alpha workstation. This is two orders of magnitude more computing time than for the 2D simulation. This leads us to the realization that 2D simulations may be very useful in characterizing significant physical effects of the process and that they should certainly be employed prior to attempting full 3D simulations. The next section describes the addition of agitation jets to the model to determine their effects.

SIMULATION OF 2D AND 3D FLOW WITH JET AGITATION, BUT NO FIBER BUILDUP OR FREE SURFACE is the second step toward full simulation of the slurry flow in the tank. The agitation produced by the air jets in the actual slurry tank was modeled using water jets to avoid the need to employ two-phase flow. To mimic the effect of the jets, the rate of momentum delivered by the air jets was matched by the momentum of the modeled water jets. The rate of momentum delivery is a function of the fluid velocity, the fluid density and the area of the openings through which the jets issue.

A two-dimensional simulation of the jet agitation model was accomplished first. In 2D, the agitation jets were, in effect, axisymmetric 'rings' of fluid issuing from the supply manifold because a two-dimensional model does not allow for discrete pinhole jets. After a number of unsuccessful attempts to get a steady-state solution to the tank flow problem with agitation jets, it was determined that the problem is an unsteady one. Apparently, the agitation jets set up a circulation loop that starts at the jets and moves upward. At some point, the water in the loop changes direction and heads radially toward the center of the tank. Before reaching the center of the tank, the loop turns downward toward the screen. At the top of the piston, the loop splits; part goes through the screen, increasing the flow of water through the outer edge of the screen, and part goes back toward the jets along the surface of the piston.

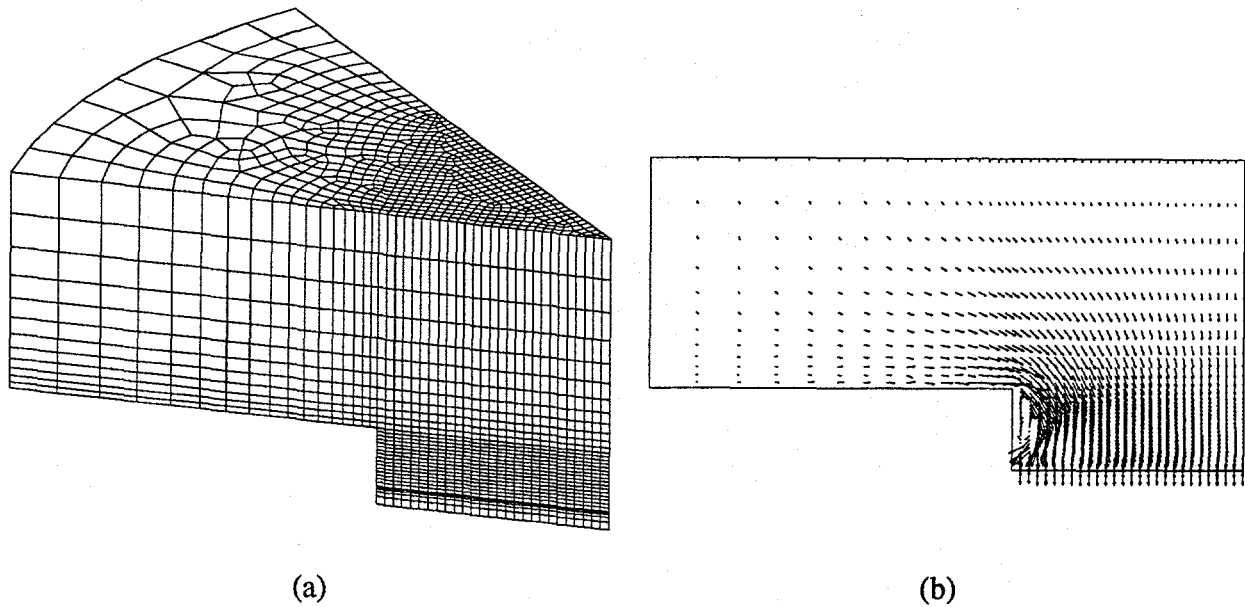


Figure 6. (a) Finite element grid and (b) velocity vector plot for 3D simulations of slurry tank for objective 1. Note recirculation zone is similar to 2D results.

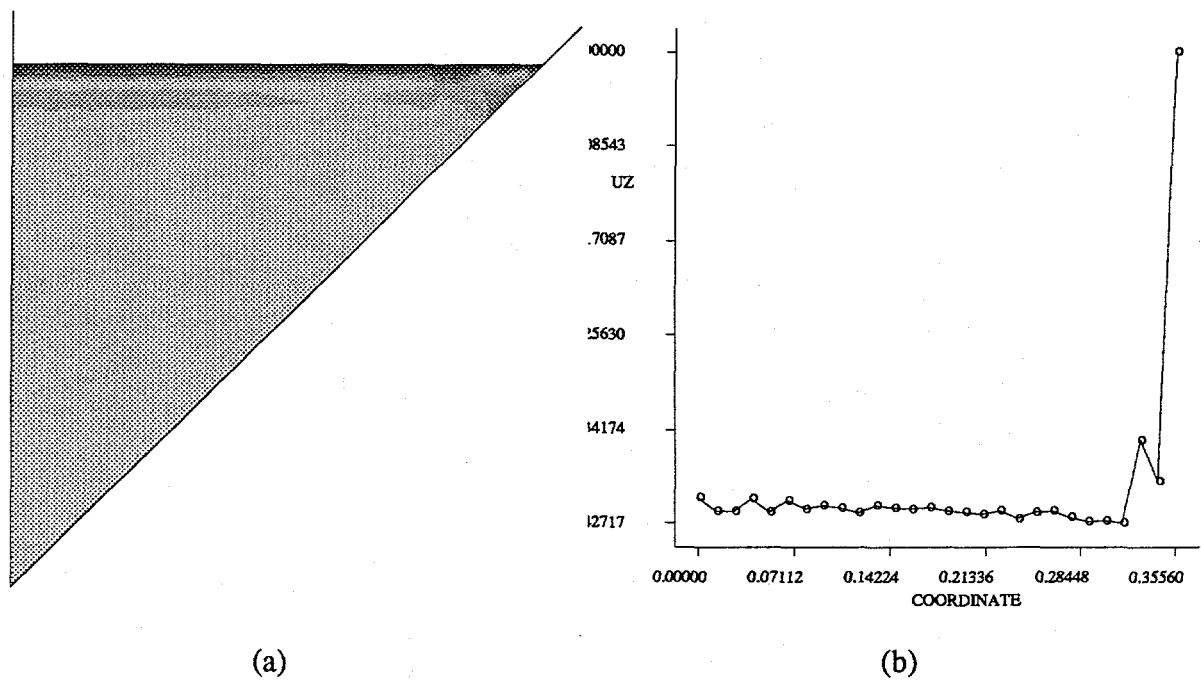


Figure 7. (a) Contour plot of axial velocity just above screen for 3D flow for objective 1. (b) Distribution of axial velocity just at the upper face of the screen along left edge of sector as seen in (a); positive flow is in negative z direction. The center of the screen is toward the left.

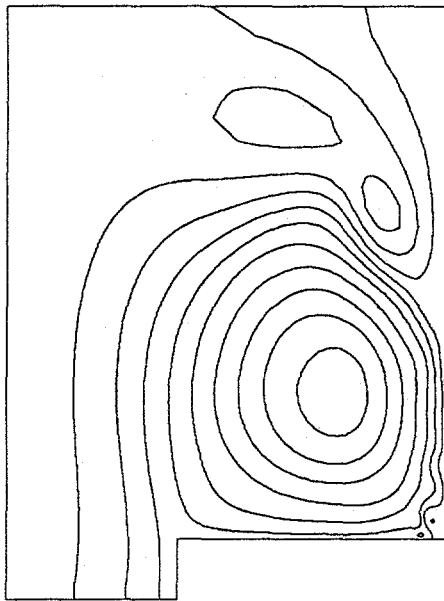
Figure 8a shows a streamline contour plot for the 2D case at time 1.78 seconds. We can see that the flow circulation loop is of relatively large size; note that the slurry tank modeled here is four feet high. Figure 8b plots the distribution of velocity just as the water reaches the screen. The center of the screen is at the left. We see that the water velocity increases about 6% from the screen center to the peak near the outer screen edge. The oscillatory nature of the profile just near the outer edge is due to the fact that the thin boundary layer there is not resolved. At the later time 3.88 sec., Figure 9a shows the streamline contour plot and corresponding circulation loop which is somewhat smaller than the previous one. The water velocity at the screen outer edge for this instant in time actually decreases from the screen centerline by about 14% as can be seen in Figure 9b. Apparently, this decrease in the water velocity is related to the destabilization of the circulation loop as it changes size and hence changes the flow pattern in the tank.

For the 3D model with jet agitation, the flow domain was restricted to a 1.2° slice of the full tank. This small size for the slice was chosen to minimize the number of cells and because it accommodated one pair of jets (each at a different radius; see Fig.1). Because the slice was so narrow, special care had to be taken to prevent the creation of highly skewed cells which are not amenable to good accuracy. Figure 10a shows a vector velocity plot for the 3D unsteady simulation at time 0.18 seconds. We can see a large circulation loop that spans the height of the model which is three feet. This shortened height greatly decreased the number of cells needed and allowed the simulation to be made in a reasonable time. Figure 10b shows the velocity profile across the screen with the screen center at the left. Again, the velocity of water is negative in the direction of flow through the screen. We see that the velocity magnitude near the outer screen edge is about 35% greater than the centerline value. This is 4 to 6 times greater than the maximum increase we saw for the 2D model above. Apparently, this discrepancy is related to the difference between having a 'ring' of jet agitation for the 2D model and discrete round jets for the 3D model.

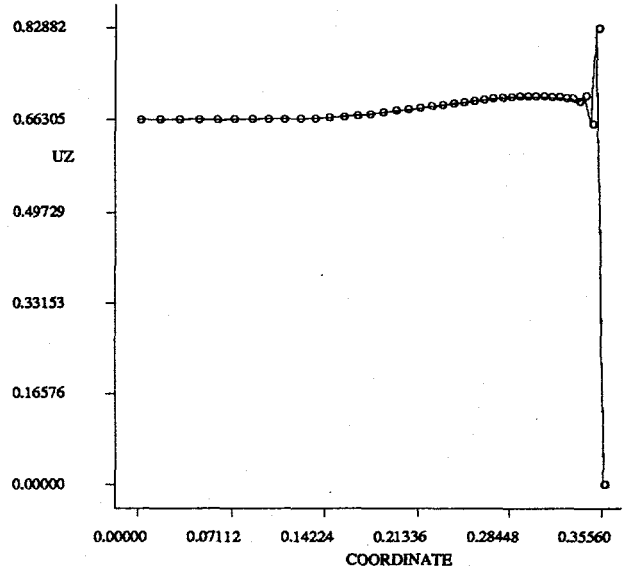
It is apparent that the agitation jets provide significant effect to the flow of the water through the screen, with both increasing and decreasing flow rates near the outer screen edge. The time-integrated flow across the screen should be computed to determine the final thickness of the fiber mat which is assumed to be proportional to the mass flow of water through the screen. However, this is superfluous at this point because both the deposition of fibers on the screen and the presence of a free surface will have significant effects on this calculation.

SIMULATION OF 2D AND 3D FLOW WITH JET AGITATION, FIBER BUILDUP WITH AND WITHOUT A FREE SURFACE are the third and fourth steps toward full simulation of the slurry flow in the tank. As of this writing, work is still underway to accomplish these objectives. The next step in accomplishing the modeling plan objectives is related to optimization of the slurry process.

OPTIMIZATION OF THE SCREEN HOLE SPACING is the next objective of the modeling plan and represents a step toward determining how to control the slurry process in order to achieve the overall goal of obtaining a fiberglass preform with a uniform distribution of material (by mass). Optimization software has been interfaced with the fluid dynamics analysis code FIDAP such that the optimizer controls calls to the analysis code and varies the distribution of permeability of the screen. The 2D model with jet agitation was implemented in the optimization study. To reduce computing time and still show feasibility, the steady-state version of the 2D model was used. Since the steady-state version of the model does not converge to a steady-state solution, a particular number of iterations were run for each analysis call which allowed the simulation to closely approach a flow pattern that exhibited one of the flow circulation loops discussed above. While the simulation did not faithfully represent the unsteady flow physics of the slurry process, it did demonstrate the feasibility of using optimization for the design of the screen. A simulation faithful to the important physics of the process is not yet available in any case.

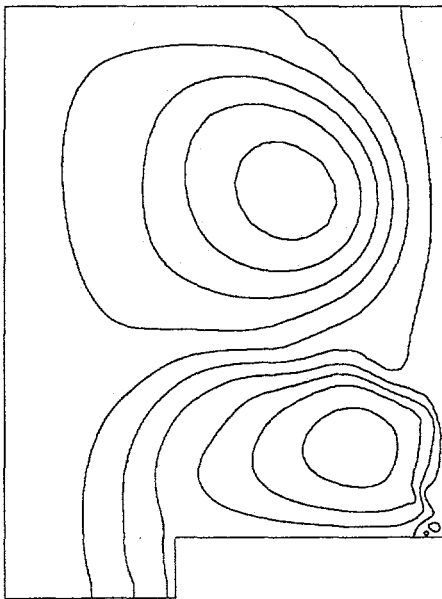


(a)

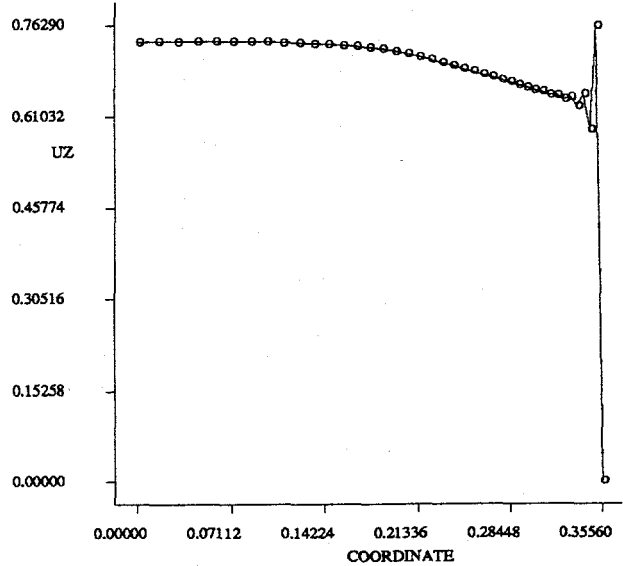


(b)

Figure 8. (a) Streamline contour plot for 2D slurry tank with jet agitation at time 1.78 seconds for objective 2. Note size of (lower) circulation loop caused by jets. (b) Line plot of water velocity just above screen at same time.

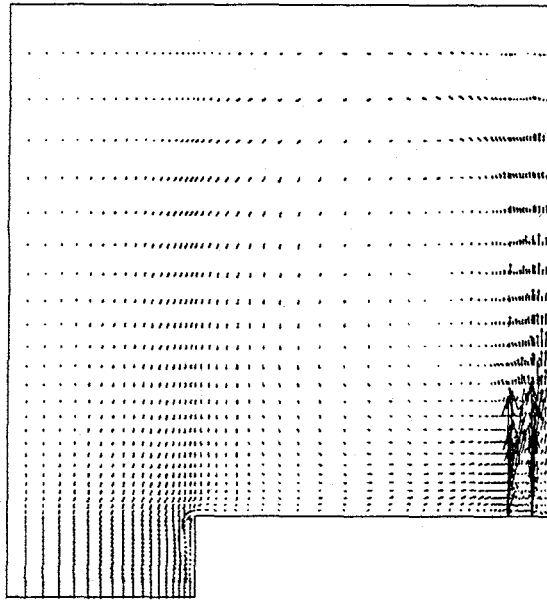


(a)

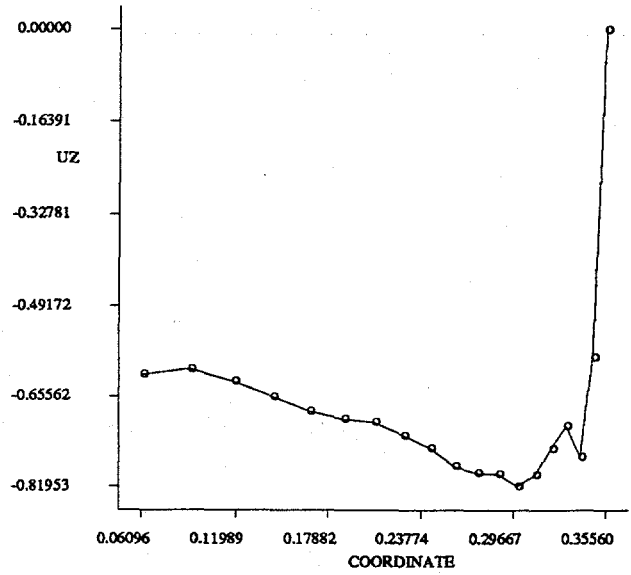


(b)

Figure 9. (a) Streamline contour plot for 2D slurry tank with jet agitation at time 3.88 seconds for objective 2. Note size of circulation loop caused by jets. (b) Line plot of water velocity just above screen at same time.

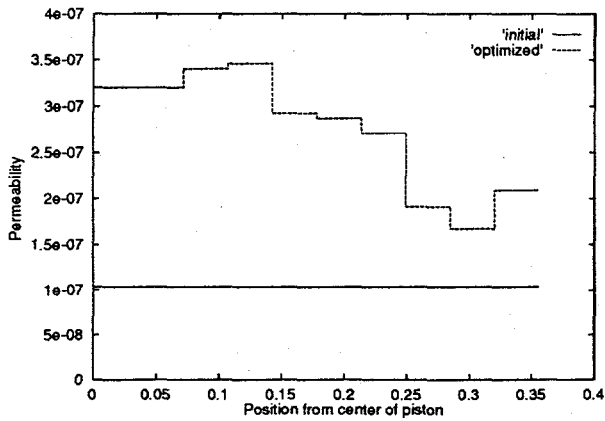


(a)

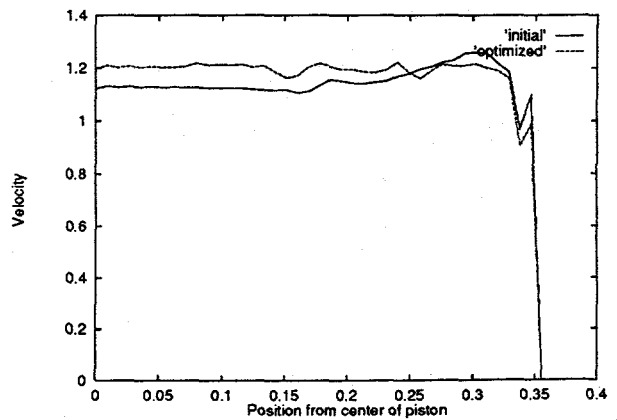


(b)

Figure 10. (a) Velocity vector plot for 3D slurry tank with jet agitation at time 0.18 seconds for objective 2. (b) Line plot of water velocity just above screen at same time.



(a)



(b)

Figure 11. (a) Distribution of permeability of slurry tank screen before and after optimization; the screen was divided into 10 segments (radially), each of which could have a different permeability. (b) Distribution of water velocity as a function of radial position for initial and optimized screen.

The initial 2D model that was optimized employed the 50% open area screen with a permeability of $1.0334 \times 10^{-7} \text{ m}^2$. The optimizer was allowed to vary the permeability of the screen within the range of open areas for which we have experimental data (23% - 72%). The initial simulation yielded a peak near the outer screen edge in water velocity having a value 12.5 % above centerline values. The screen in the 2D model was segmented into ten intervals such that each interval could have a different value of permeability, although the permeability would have to be constant for the length of each segment and then change abruptly to a new value at the segment boundary. Figure 11a presents the results of the permeability optimization of the screen. We see that the percentage open area is relatively lower near the outer edge where the peak water velocity occurred. Figure 11b illustrates the distributions of water velocity for the original model with constant open area and for the optimized screen. We see that the variation in water velocity has diminished to 0.5 % (excluding the region adjacent to the outer screen edge where the velocity is forced to zero). From Figure 11b we see that there are still small jumps in the water velocity for the optimized screen; these are due to the abrupt change in open area between segments. Clearly, the screen could be subdivided further to smooth these jumps; however, the potential for optimal screen design has been demonstrated. The final objective in the modeling plan has yet to be accomplished.

SUMMARY

We are in the process of developing a computer model using a commercial fluid dynamics code to analyze the flow of water in a slurry tank to be used to create fiberglass preforms in complex shapes for the manufacture of automobile components. The slurry tank consists of a hydraulic piston with a screen mounted in its center. The piston is driven upwards through the tank, collecting fiberglass on the screen. Air jets around the periphery of the piston mix the slurry, keeping the fiberglass from settling. We have devised a plan to model a simplified version of the true flow process, hoping to be able to avoid complicated physics that are not well understood and may be unimportant to the overall process. Our plan simplifies the transient, multiphase, multicomponent flow of the slurry to a transient, single-phase, single-component flow. The plan envisions the step by step incorporation of jet agitation (using water instead of air jets), fiber deposition and buildup (using a porous medium model having a time-varying thickness) and inclusion of a free surface (which changes position with time) to an initial model that effectively treats the flow as pipe flow with an obstruction. We have accomplished half of the project objectives, learning more each time about effects that potentially dominate the flow. We have also applied an optimizing algorithm to the design problem of determining the optimal screen open area distribution to force the water to have a spatially uniform flow rate through the screen.

ACKNOWLEDGEMENTS

This work was performed at the Idaho National Engineering Laboratory (INEL) under the auspices of the U.S. Dept. of Energy (DOE), Idaho Operations Office, Contract No. DE-AC07-94ID13223 with the help of Claude A. Di Natale and Gerald J. Cinpinski of the Automotive Composites Consortium and Bruce N. Greve of The Budd Company. We also acknowledge the help and support of INEL personnel Glenn A. Moore, Carl M. Stoots and Gregory A. Hulet.

REFERENCES

1. A. Baloch and M. F. Webster, "A Computer Simulation of Complex Flows of Fibre Suspensions," *Computers & Fluids*, Vol. 24, No. 2, pp. 135-151, 1995.
2. M. Kaviany, Principles of Heat Transfer in Porous Media, Springer-Verlag, New York, 1991.